

Microstructural effects of high-energy grinding on poorly soluble drugs: the case study of efavirenz

Elisa Cappelletto,^{1,a)} Luca Rebuffi,² Alberto Flor,¹ and Paolo Scardi¹

¹Department of Civil, Environmental and Mechanical Engineering, University of Trento, via Mesiano 77, 38123 Trento, Italy

²Eletra-Sincrotrone Trieste, Area Science Park, Basovizza, 34149 Trieste, Italy

(Received 14 October 2016; accepted 21 January 2017)

In this work, a poorly water-soluble drug (efavirenz) was mechanically activated by ball-milling. The effect of the mechanical activation on the dissolution behavior was investigated considering changes in the particle size and morphology. The powder diffraction was used to follow the comminution process, verifying phase compositions, and crystalline domain size. The interplay between domain and grain size was studied in relation to the solubility rate, through specific dissolution tests. Finally, the morphological characterization has allowed to complete the physical–chemical characterization of the milled powders. This study demonstrated that the mechanical activation of the drug leads the particle size reduction and, with a long milling time, morphological changes. The grain size reduction is not always sufficient to increase the solubility: morphology and agglomeration grade play an important role in the dissolution process. © 2017 International Centre for Diffraction Data. [doi:10.1017/S0885715617000161]

Key words: Efavirenz, nanosizing, crystalline domain size, comminution processes, dissolution, ball milling

I. INTRODUCTION

Efavirenz (EFV), (4S)-6-chloro-4-(cyclopropylethynyl)-4-(trifluoromethyl)-1,4-dihydro-2H-3,1 benzoxazin-2-one, a non-nucleoside reverse transcriptase inhibitor (NNRTI) of the HIV-1 (human immunodeficiency virus type 1), is a crystalline lipophilic solid with a poor aqueous solubility [$0.9 \mu\text{g ml}^{-1}$] and a low intrinsic dissolution rate [categorized as a class 2 drug under the BCS (Biopharmaceutics Classification System)] (Mahapatra and Murthy, 2014; Tandel *et al.*, 2015). The poor solubility of the pharmaceutical compounds decreases the bioavailability *in vivo* owing to their low dissolution rate in the gastrointestinal fluids following oral administration. Instead, an appropriate dissolution rate is necessary for attaining proper oral drug therapy, as high dosages often imply adverse effects on the patient. The improvement of the solubility is a major challenge for the pharmaceutical community, faced by several approaches such as physical and chemical modifications, preparing solid dispersions, complexation, solubilization, and salts formulations (Assis da Costa *et al.*, 2013; Campos de Melo *et al.*, 2013; Kolhel *et al.*, 2014). Among the physical methods, particle size reduction is a known strategy for improving solubility of drugs, which is intrinsically related to drug particle size by the Noyes–Whitney Eq. (1) (Sun *et al.*, 2012; Sinha *et al.*, 2013; Chogale *et al.*, 2016):

$$\frac{dm}{dt} = \frac{D}{d.A.} (C_s - C_t), \quad (1)$$

where dm/dt is the solute dissolution rate, D is the diffusion coefficient, d is the thickness of the concentration, A is the surface area

of the solute particle, C_s is the particle surface (saturation) concentration, and C_t is the concentration in the bulk solvent/solution.

Several technologies allow the production of ultrafine particles down to the micrometric scale (micronization) (Rasenack and Muller, 2003), but when drug solubility is very low, down-sizing to the micrometer range can be insufficient to increase dissolution rate and gastrointestinal absorption (Dizaj *et al.*, 2015; Loh *et al.*, 2015). In the past decade, significant improvement in comminution processes (air jet milling, ball milling, vibration milling, etc.) has made possible the production of submicron-sized drugs by exploiting mechanical energy to physically break down coarse particles (Hansa *et al.*, 2015). Since, the micro and nanoparticles produced by milling have a large surface area, increased free energy and decreased thermodynamic stability, they tend to agglomerate. Effective surface area is thus reduced, leading to a decrease in the dissolution rate and bioavailability, which becomes comparable or even lower than in the untreated counterparts. Hence, the pharmaceutical compounds are often co-milled together with additives (stabilizers) to minimize the conditions promoting aggregation. The purpose of this work is to study the effect of size and morphology on the dissolution profile after the mechanical activation. High-energy ball milling was used on pre-micronized EFV, with or without polyvinylpyrrolidone (PVP) as adjuvant, for increasing milling time. Powder diffraction was used to follow the comminution process, verifying phase compositions and the crystalline domain size by line profile analysis. The interplay between domain and grain size was studied in relation to the solubility rate, through specific dissolution tests both on powder and tablet. Scanning electron microscopy (SEM) was used to study the morphology of the mechanically activated powder. Synchrotron radiation X-ray computed

^{a)} Author to whom correspondence should be addressed. Electronic mail: elisa.cappelletto@unitn.it

TABLE I. Samples produced with different milling parameters.

Sample	Milling time	Additive (50% w/w%)
EP430	30 min	
EP41	1	
EP46	6	
PEP430	30 min	PVP
PEP41	1	PVP
PEP46	6	PVP

microtomography (SR- μ CT), a non-destructive technique, was employed to follow the process of dissolution of the tablets.

II. EXPERIMENTAL

A. Materials

The starting active pharmaceutical ingredient (API) was kindly donated by the Brazilian Farmanguinhos-FIOCR UZ, a governmental pharmaceutical laboratory. The EFV raw material, a micronized polymorph I phase, was subjected to high-energy grinding in a planetary ball mill, under conditions reported in Table I. PVP K-10 was added to minimize the agglomeration of EFV particles via steric mechanism: long-chain polymers are absorbed onto the surfaces of the drug particles, forming a physical barrier that prevents the close approach of the particles.

B. Methods

X-ray diffraction patterns of the milled samples were collected at the MCX beamline (Elettra Sincrotrone Trieste), with a photon energy of 8 KeV (corresponding to $\lambda = 0.15498$ nm) and an angular range from 2° to 24° in 2θ . Measurements were performed in Debye–Scherrer geometry, filling standard Kapton™ capillaries with EFV samples, and results qualitatively correlated with the database of crystal structures – CIF [Crystallographic information file, CCDC site (Chadha, Leuner, Mahapatra)] for phase identification. Microstructural parameters were obtained by Line Profile Analysis of the XRPD (X-ray powder diffraction) patterns, using the software PM2K implementing the Whole Powder Pattern Modelling

(WPPM) approach (Scardi *et al.*, 2010; Rebuffi *et al.*, 2014). Dissolution tests were performed both on powder and tablet samples by using an Erweka DT-626 dissolutor (six vessels) with a paddle apparatus (described as apparatus 2 in the US Pharmacopeia). The dissolution procedure consisted of placing a known amount of the drug (powder or tablet) into the dissolution vessel. Dissolution conditions were 900 ml of methanol solution (40% V/V) at $37 \pm 0.5^\circ\text{C}$, with a rotation speed of 50 rpm. The drug release was simultaneously analyzed by an UV–Vis Spectrophotometer (Perkin Elmer Lambda 650) coupled with the dissolutor. Samples were collected in continuous using a 40 μm cannula filter; the analysis was performed at 248 nm wavelength. Morphological evaluation was performed by SEM [ZEISS Field Emission (FE) SEM Supra 40, CNR-IOM Trieste]. Samples were mounted with carbon adhesive onto an aluminum holder, and photographed at a voltage of 1 kV. SR- μ CT tomographic images were acquired at the SYRMEP beamline of Elettra Sincrotrone Trieste (Trieste, Italy) (Tromba *et al.*, 2010). Samples were scanned with synchrotron radiation at 20 keV. The pixel size was 2 μm and the exposure time was 1 s. For each acquisition, 1800 projection images were taken. The projection sets of tablet for each time point of dissolution (0, 3, 6, 24 h) were reconstructed using ImageJ software (Schneider *et al.*, 2012).

III. RESULTS

Powder diffraction clearly shows the effect of the comminution process on polymorph I EFV, with a particle size reduction observed for long milling time (Figure 1). This trend is maintained also with the addition of the stabilizing agent that prevents the agglomeration. The morphology of the mechanically activated samples was investigated by the SEM analysis. Micronized EFV (raw material) is characterized by rod-like grains (columnar crystals) typical of the polymorph I [Figure 2(a)] (Costa Pinto *et al.*, 2014). Short milling time does not change the morphology [Figures 2(b) and 2(c)], which on the contrary appears different after 6 h of grinding. EP46 shows needle-shaped crystals [Figure 2(d)], whereas by adding the stabilizer crystal shape is preserved: particles show the same morphology as the starting material even after a prolonged grinding [Figure 2(f)]. The dissolution profiles of the activated samples, obtained using the powder

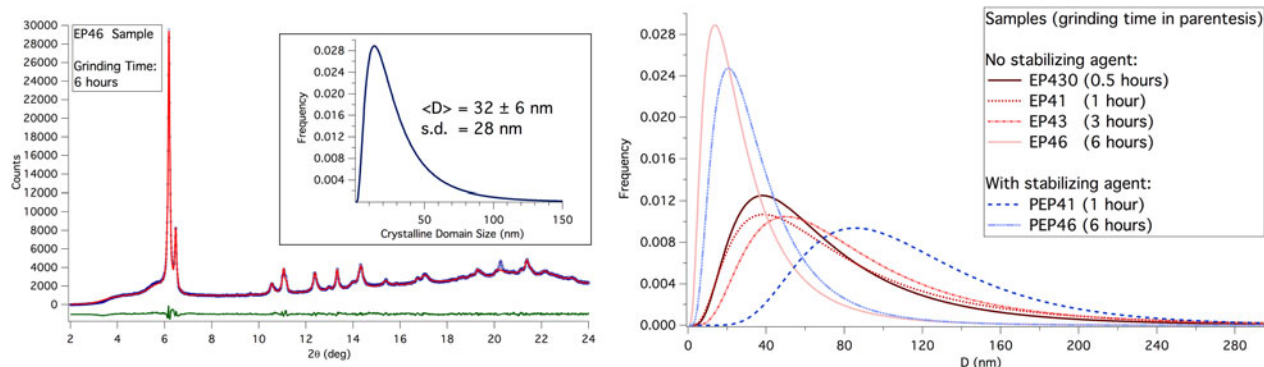


Figure 1. (Colour online) Powder diffraction data (dot) of sample EP46, and corresponding WPPM result (line), with difference (residual, line below); inset shows the corresponding domain size distribution. Domain size distributions obtained by WPPM are shown on the right for all samples of this study.

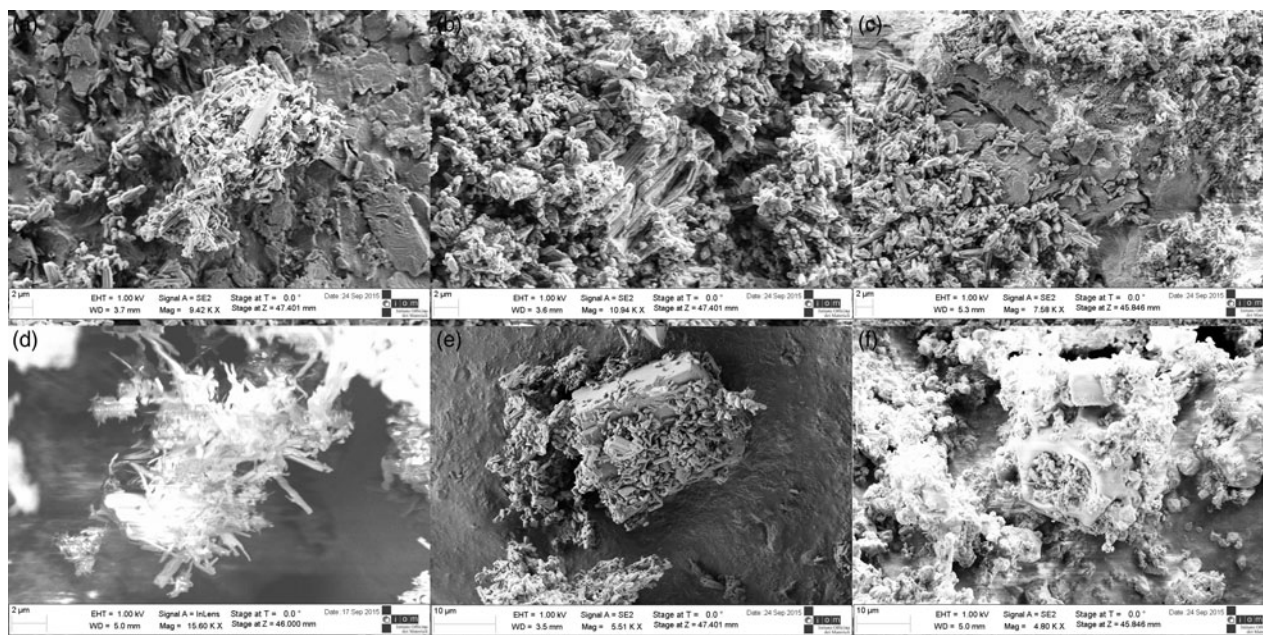


Figure 2. SEM micrographs of EFV micronized (a), EP430 (b), EP41 (c), EP46 (d), PEP41 (e), and PEP46 (f).

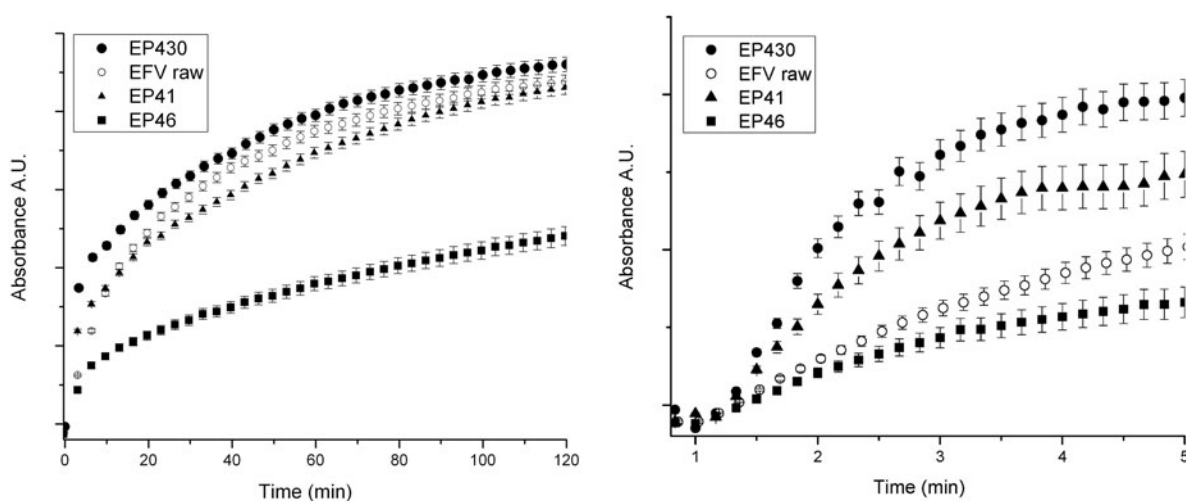


Figure 3. Dissolution profiles of micronized efavirenz (EFVraw) and milled samples by powder dissolution method (left); early stages of the dissolution process (right).

dispersion method, are presented in Figure 3. A long grinding time, EP46, yielded a worsening of the dissolution behavior in comparison with the micronized raw material, EFV. A higher percentage of dissolved drug was observed with the shortest comminution process (EP430, 30 min). On long-term, EP430 and EP41 present dissolution profile close to the sample not mechanically activated, although the same samples show a higher dissolution efficiency in the first minutes of test [Figure 3(right)]. Figure 4 shows the dissolution profiles of samples with PVP, which does not absorb at this specific wavelength. The presence of the superdisintegrant involves a rapid solubilization followed by a similar plateau for each sample (that was maintained for all the period of analysis). X-ray computed tomography (CT) allows a rapid analysis of the internal structure during the dissolution process (Figure 5). The non-invasive measurements were carried out

on tablets and the three-dimensional (3D) reconstruction, obtained from the high-resolution X-ray CT images, compared with the dissolution profiles (Figure 6). The micronized EFV tablet revealed a similar dissolution profile to the ground sample (EP430); in fact, both their compressed powders are characterized by a dense structure that dissolves very slowly, so that the curves do not reach a plateau even after 24 h in the dissolution medium. As seen with the powder samples, adding PVP enhances the dissolution profile of the API, reaching a plateau after 24 h. Most notably, PEP43 dissolution process is associated with a fine structure almost free of agglomerates.

IV. DISCUSSION

Results presented in this work point out that a simple size reduction is not sufficient to increase the dissolution profile of

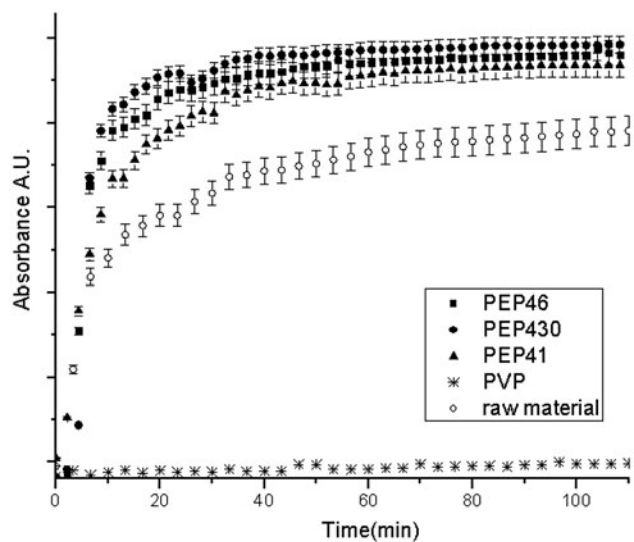


Figure 4. Dissolution profiles of EFV, PVP K-10, and the binary systems at different milling periods.

EFV. Powder diffraction demonstrates the effectiveness of planetary ball milling in reducing the crystalline domain size after relatively long milling times (from ≈ 100 nm of starting EFV to ≈ 50 nm of EP46), but SEM investigations show that long milling periods imply changes in the grain morphology and, most probably, a recrystallization of the raw material. Nevertheless, the XRD (X-ray diffraction) analysis has not point out any polymeric changes as a result of the milling process. In general, the recrystallization process leads to the production of a different crystalline form and/or to the purification of the drug, and it was often used to improve the bioavailability of the APIs. Moreover, Figure 7 suggests that, apparently, the recrystallization is not always associated with an increase of solubility: there is a worsening of the profile following a recrystallization process, which involved a change in the morphology of the grains similar to that obtained after extensive grinding. A relatively short grinding (EP430) seems to improve slightly the dissolution of the EFV. The effect is most evident in the first few minutes where the mechanical activation seems to improve dissolution [Figure 3(right)]. A

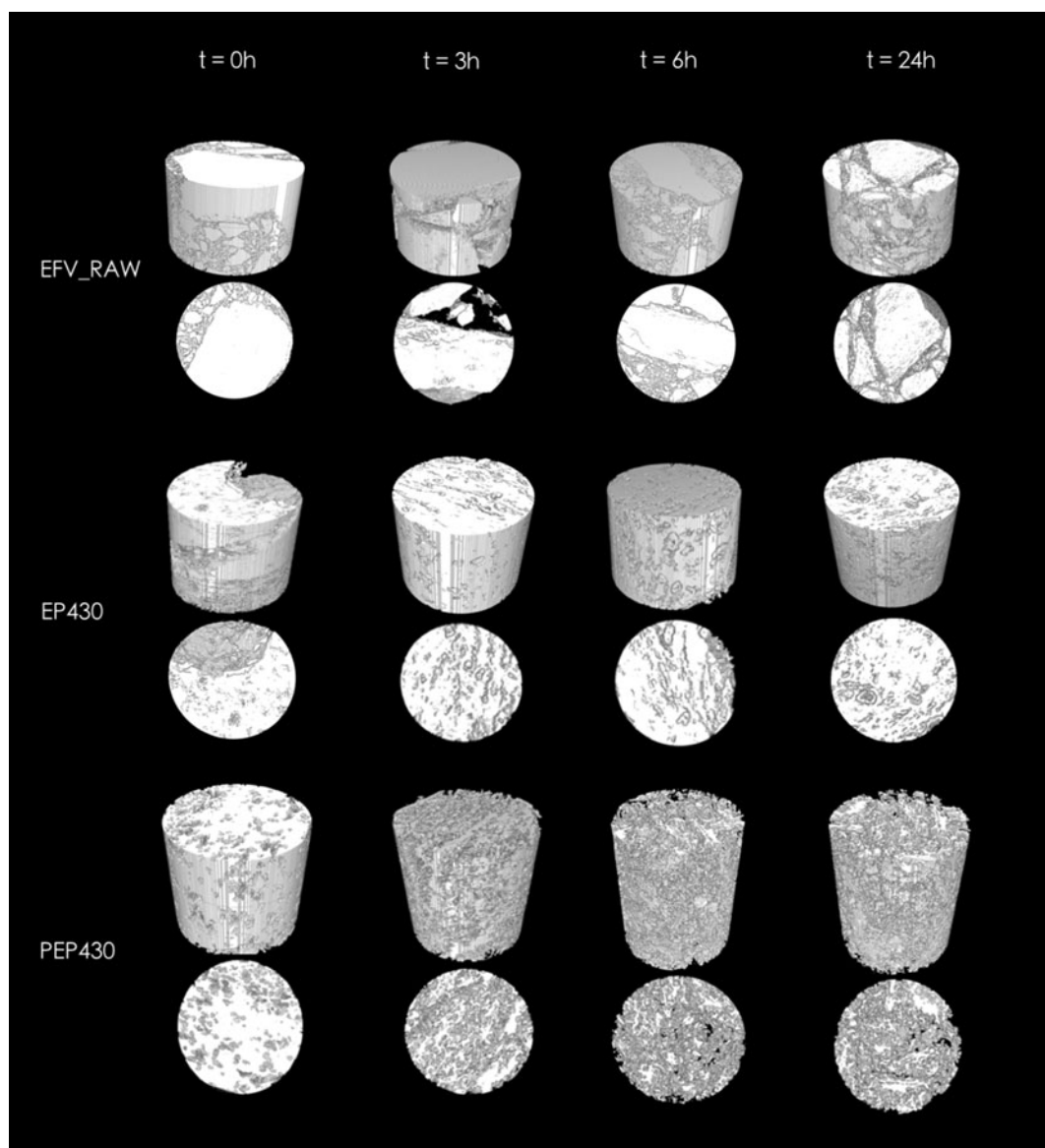


Figure 5. 3D reconstructions of the SR- μ CT images.

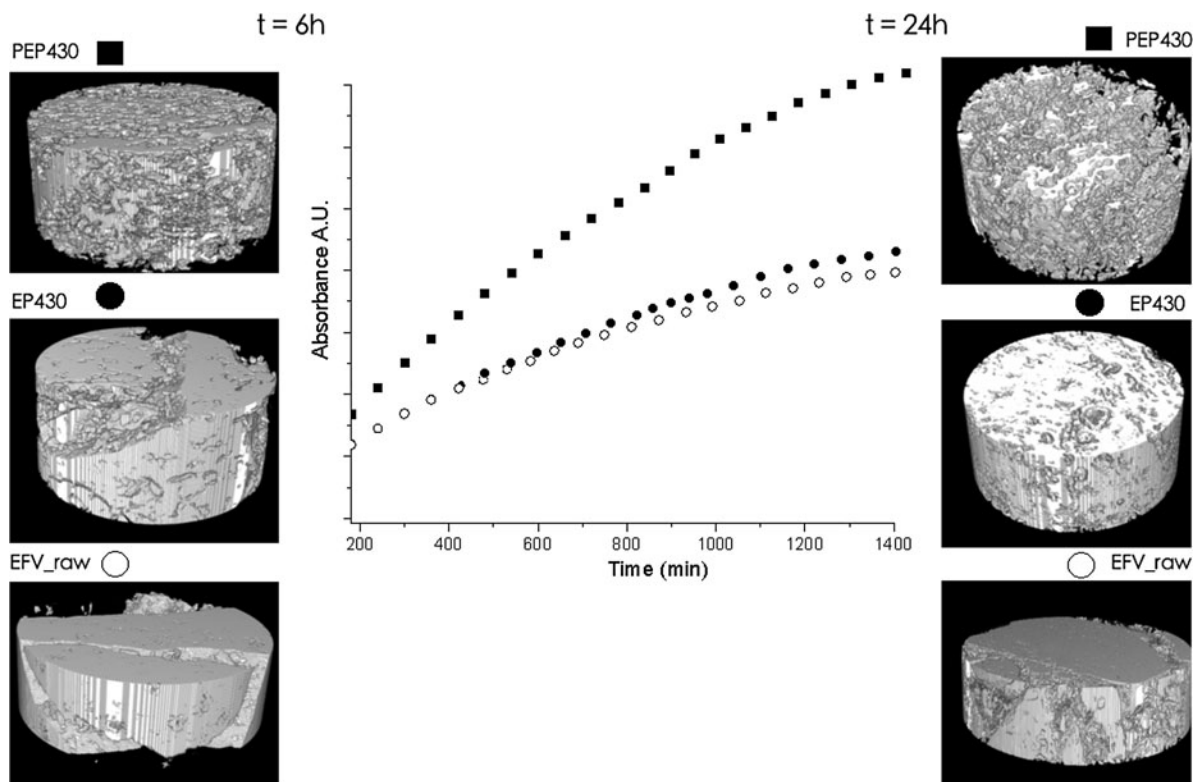


Figure 6. HR X-ray CT images compared with the dissolution test of tablet samples.

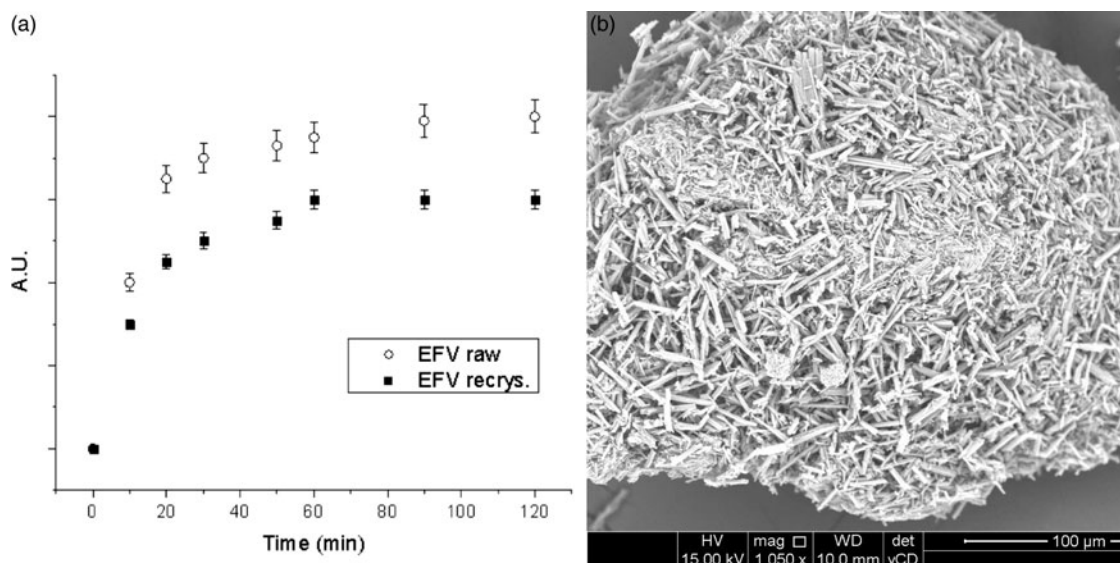


Figure 7. Dissolution profiles of EFV raw and a recrystallized sample (a) and SEM micrograph of the latter (b).

decline in the dissolution behavior is observed when the comminution process is extended; the curve of EP41 is characterized by a rapid initial dissolution followed by a plateau similar to that obtained with the raw material. The SEM micrographs show a nanostructuring (nanosizing) after grinding, not involving a change of morphology for these specific samples (Figure 2). Since nanoparticle agglomeration can worsen the dissolution profile, a stabilizing agent was added to the API. The long chains of PVP prevent the close approach of EFV particles by forming a physical barrier. Steric stabilization

was confirmed by the SR- μ CT tomographic images: following the addition of the additive, we observed a lower degree of agglomeration, and a finer structure able to improve the dissolution process. This work revealed that particle shape is also relevant to the dissolution behavior. The effect of particle shape is especially pronounced for materials with grains, which deviate markedly from sphericity (Mosharraf and Nystrom, 1995; Sun *et al.*, 2012). The present results confirm that irregular particles have a smaller dissolution rate; this seems to be related to the effect of hydrodynamic boundary

layer thickness (hH) on this process. Particle size reduction implies in an increase of the dissolution rate not only by exhibiting a large interfacial surface area, but also by decreasing the thickness of the diffusion layer around each particle. Considering that, hH can be expressed as:

$$hH = k(L'/2/V \sim /2), \quad (2)$$

where L is the length of the surface in the direction of flow, k is a constant, and V is the relative velocity of the flowing liquid against the flat surface.

Along the lines of evidence presented in this work, previous studies suggested that long, flaky particles with a high degree of irregularity may cause an increase in the average hydrodynamic boundary layer thickness, by increasing parameter L (Mosharraf and Nystrom, 1995).

V. CONCLUSION

Dissolution of drug is the rate determining step for oral absorption of poorly water-soluble drugs. According to the Noyes–Whitney equation, decrease in particle size should lead to an enhancement in solubility. Ball-milling technology is by far the most frequently used method for the production of drug nanocrystals in the pharmaceutical industry. The mechanical activation of EFV was investigated considering the effects on size and morphology of the drug's particles. Contrary to expectations, the dissolution profiles suggest that a decrease of crystalline domains does not directly implies an improvement of the dissolution behavior. In fact, the solubility depends on size, agglomeration grade, and shape of the nanocrystals. The present work is a first step in the direction of controlling the milling process so to improve EFV dissolution. Results clearly show that besides the comminution process, morphology and the agglomeration of the ground material also need to be properly controlled.

ACKNOWLEDGEMENTS

This work was funded by Project 2013-0247, "Mechanical activation to improve bioavailability and to reduce adverse effects of drugs in the therapy of chronic diseases", Fondazione Caritro, Trento. The authors thank Farmanguinhos/Fiocruz for providing the raw materials, and the MCX beamline of the Italian synchrotron Elettra for collaboration.

Assis da Costa, M., Cardoso Seiceira, R., Rangel Rodrigues, C., Rodrigues Drago, C., Mendes Cabral, L., and Antunes Rocha, H. V. (2013). "Efavirenz dissolution enhancement I: co-micronization," *Pharmaceutics* **5**, 1–22.

Campos de Melo, A. C., Ferreira de Amorim, I., de Lima Cirqueira, M., and Martins, F. T. (2013). "Toward novel solid-state forms of the anti-HIV drug efavirenz: from low screening success to cocrystals engineering strategies and discovery of a new polymorph," *Cryst. Growth Des.* **13**, 1558–1569.

Chogale, M. M., Ghodake, V. N., and Patravale, V. B. (2016). "Performance parameters and characterizations of nanocrystals: a brief review," *Pharmaceutics* **8**(26), 1–18.

Costa Pinto, E., Mendes Cabral, L., and Pereira de Sousa, V. (2014). "Development of a discriminative intrinsic dissolution method for efavirenz," *Dissolution Technol.* **21**, 31–40.

Dizaj, S. M., Vazifehasl, Z., Salatin, S., Adibkia, K., and Javadzadeh, Y. (2015). "Nanosizing of drugs: effect on dissolution rate," *Res. Pharm. Sci.* **10**(2), 95–108.

Hansa, D., Giacobbe, C., Perisutti, B., Voinovich, D., Grassi, M., Cervellino, A., Masciocchi, N., and Guagliardi, A. (2015). Nanostructured drugs embedded into a Polymeric Matrix: Vinpocetine/PVP Hybrid investigated by Debye Function Analysis, *Molecular Pharmaceutics*. **13**(9), 3024–3042.

Kolhe, S., Chaudhari, P. D., and More, D. (2014). "Dissolution and bioavailability enhancement of efavirenz by hot melt extrusion technique," *J. Pharm.* **4**(5), 2319–4219.

Loh, Z. H., Samanta, A. K., and Heng, P. W. S. (2015). "Overview of milling techniques for improving the solubility of poorly water-soluble drugs," *Asian J. Pharm. Sci.* **10**, 255–274.

Mahapatra, A. K. and Murthy, P. N. (2014). "Solubility and dissolution rate enhancement of efavirenz by inclusion complexation and liquid anti-solvent precipitation technique," *J. Chem. Pharm. Res.* **6**(4), 1099–1106.

Mosharraf, M. and Nystrom, C. (1995). "The effect of particle size and shape on the surface specific dissolution rate of micro-sized practically insoluble drugs," *Int. J. Pharm.* **122**, 35–47.

Rasenack, N. and Muller, B. W. (2003). "Micron-size drug particles: common and novel micronization techniques," *Pharm. Dev. Technol.* **9**(1), 1–13.

Rebuffi, L., Plaisier, J. R., Abdellatif, M., Lausi, A., and Scardi, P. (2014). "MCX: a synchrotron radiation beamline for x-ray diffraction line profile analysis," *Z. Anorg. Allg. Chem.* **640**, 3100–3106.

Scardi, P., Ortolani, M., and Leoni, M. (2010). "WPPM: microstructural analysis beyond the Rietveld method," *Mater. Sci. Forum* **651**, 155–171.

Schneider, C. A., Rasband, W. S., and Eliceiri, K. W. (2012). "NIH image to imageJ: 25 years of image analysis," *Nat. Methods* **9**(7), 671–675.

Sinha, B., Muller, R. H., and Moschwitz, J. P. (2013). "Bottom-up approaches for preparing drug nanocrystals: formulations and factors affecting particle size," *Int. J. Pharm.* **453**(1), 126–141.

Sun, J., Wang, F., Sui, Y., She, Z., Zhai, W., Wang, C., and Deng, Y. (2012). "Effect of particle size on solubility, dissolution rate, and oral bioavailability: evaluation using coenzyme Q10 as naked nanocrystals," *Int. J. Nanomed.* **7**, 5733–5744.

Tandel, H., Patel, P., and Jani, P. (2015). "Preparation and study of efavirenz microemulsion drug delivery system for enhancement of bioavailability," *Eur. J. Pharm. Med. Res.* **2**(5), 1156–1174.

Tromba, G., Longo, R., Abrami, A., Arfelli, F., Astolfo, A., Bregant, P., Brun, F., Casarin, K., Chenda, V., Dreossi, D., Hola, M., Kaiser, J., Mancini, L., Menk, R. H., Quai, E., Quai, E., Rigon, L., Rokvic, T., Sodini, N., Sanabor, D., Schultke, E., Tonutti, M., Vascotto, A., Zanonati, F., Cova, M., and Castelli, E. (2010). "The SYRMEP beamline of elettra: clinical mammography and bio-medical applications," *AIP Conf. Proc.* **1266**(1), 18–23.